

Dalton Transactions

Accepted Manuscript



This is an *Accepted Manuscript*, which has been through the Royal Society of Chemistry peer review process and has been accepted for publication.

Accepted Manuscripts are published online shortly after acceptance, before technical editing, formatting and proof reading. Using this free service, authors can make their results available to the community, in citable form, before we publish the edited article. We will replace this *Accepted Manuscript* with the edited and formatted *Advance Article* as soon as it is available.

You can find more information about *Accepted Manuscripts* in the [Information for Authors](#).

Please note that technical editing may introduce minor changes to the text and/or graphics, which may alter content. The journal's standard [Terms & Conditions](#) and the [Ethical guidelines](#) still apply. In no event shall the Royal Society of Chemistry be held responsible for any errors or omissions in this *Accepted Manuscript* or any consequences arising from the use of any information it contains.



Journal Name

ARTICLE

Analysis of the electrostatics in Dy^{III} single-molecule magnet: the case study of Dy(Murex)₃

Received 00th January 20xx,
Accepted 00th January 20xx

DOI: 10.1039/x0xx00000x

www.rsc.org/

J. Jung,^a X. Yi,^b G. Huang,^b G. Calvez,^b C. Daiguebonne,^b O. Guillou,^b O. Cador,^b A. Caneschi,^d T. Roisnel,^a B. Le Guennic^{a*} and K. Bernot^{b*}

A Dy^{III}-based single-molecule magnet is reported. *ab initio* calculations highlight that molecular symmetry plays a predominant role over site symmetry in determining the shape and orientation of Dy^{III} magnetic anisotropy. Moreover the dipolar component of the electrostatic potential created by the surrounding ligands is shown to be the driving force of its magnetic behaviour.

Introduction

In the past decade the use of lanthanide ions in coordination chemistry¹ has permitted the design of a tremendous amount of compounds² with properties as diverse as luminescence,³ porosity,^{3e, 3f} catalytic activity,⁴ temperature⁵ or chemical sensors,^{3f} or some of them combined into hybrid materials⁶. They are also expected to show magneto-chiral dichroism, has observed on chains based on anisotropic 3d ions.⁷ Their strong magnetic anisotropy also allowed the observation of single-molecule magnet (SMM) behaviour⁸ even on mononuclear compounds.⁹ In such molecules, lanthanide ions have been associated to a wide variety of ligands^{8a} that produce different electrostatic environments around the magnetic centre that strongly impact their magnetic behaviour.¹⁰ In a previous work we used historic bio-inspired ligand, the murexide (ammonium salt of 2,6-dioxo-5-[(2,4,6-trioxo-5-hexahydropyrimidinylidene)amino]-3H-pyrimidin-4-olate) that has a great affinity for lanthanide ions and is widely used in complexometric studies.¹¹ We have been able to isolate the compound of formula Yb(Murex)₃·11H₂O.¹² Its SMM behaviour was rationalized thanks to low temperature near infra-red emission.

In the present work we study the Dy^{III} derivative of this family of compounds, which after great synthetic efforts was obtained as single-crystals. We focus our investigation on the influence of the (N₃O₆) coordination environment on the lanthanide magnetic properties. From the theoretical point of view such investigation can be performed by means of *ab initio* SA-CASSCF/RASSI-SO calculations. Analysis of the resulting

atomic point charges distribution around the magnetic centre permits to rationalize the ground state magnetic anisotropy of the lanthanide ion.¹³ However, in the present case, the peculiar geometry of the compound hampers this simple treatment. It forces us to adopt a more detailed analysis of the electrostatics potential around the Dy^{III} ion. This approach highlights the predominant contribution of the dipolar moments held by ligands atoms.

Results and discussion

Reaction of Dy(NO₃)₃·6H₂O and murexide affords a reddish suspension from which crystals of good quality can be isolated. The resulting compound is isostructural with the already reported Yb^{III} derivative of formula Yb(Murex)₃·11H₂O.¹² It crystallizes in the Pccn space group (N°56), with Z=4 (Tables S1, S2 and S3). The Dy^{III} ion is nine coordinated in a (N₃O₆) environment by three tridentate anionic murexide ligands to form a neutral Dy(Murex)₃·xH₂O complex (**1**) (Figure 1). Each complex is well isolated with a minimum Dy-Dy distance of 9.85 Å (Figures S1, S2 and S3). Numerous water molecules have been found in the crystal packing, but contrary to the Yb^{III} derivative, are too disordered to be reasonably taken into account in refinement procedure.

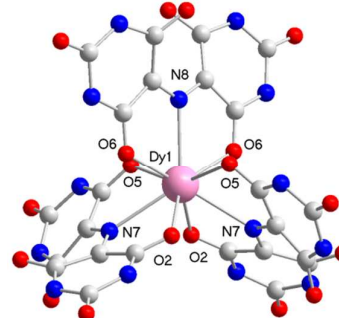


Figure 1: Representation of Dy(Murex)₃·xH₂O with labelling scheme. Hydrogen atoms omitted for clarity.

^a Address here.

^b Address here.

^c Address here.

† Footnotes relating to the title and/or authors should appear here.

Electronic Supplementary Information (ESI) available: [details of any supplementary information available should be included here]. See DOI: 10.1039/x0xx00000x

Static magnetic properties (dc) have been investigated. At room temperature $\chi_M T$ value is 14.04 emu.mol.K⁻¹, in agreement with the expected 14.17 emu.mol.K⁻¹ (Figure 2). A continuous decrease of $\chi_M T$ is seen as the temperature is lowered, because of the depopulation of sublevels of the ground state manifold.^{8d}

Commonly $\chi_M T$ vs T curves are reproduced by modelling crystal-field effects with the extended Stevens operators technique.¹⁴ However such procedure implies geometric approximation of the metal centre symmetry. Indeed, on the Yb^{III} derivative, the magnetic behaviour was nicely reproduced by considering a D_{3h} site symmetry arising from the six oxygen atoms of the first coordination sphere.¹² Similar approximation is legitimated on **1** by the very close Dy-O (2.344 to 2.375 Å) and Dy-N distances (2.570-2.573 Å) (Table S2). With the Hamiltonian: $\hat{H} = B_2^0 O_2^0 + B_2^2 O_2^2 + B_4^0 O_4^0 + B_4^2 O_4^2 + B_6^0 O_6^0 + B_6^2 O_6^2$ the experimental curve can be well reproduced (R=0.99997) with the following parameters: $B_2^0 = 0.2215$ cm⁻¹, $B_4^0 = 3.039 \times 10^{-3}$ cm⁻¹, $B_6^0 = 5.76 \times 10^{-5}$ cm⁻¹ and $B_6^2 = 1.75 \times 10^{-4}$ cm⁻¹ (Figure 2). Field variation of the magnetization at 2 K is also well reproduced with these parameters (inset Figure 2). The ground state is found to be a mixture of different M_J eigenstates with the main contribution coming from the $M_J = \pm 13/2$. The total splitting of the ⁶H_{15/2} ground multiplet is 220 cm⁻¹ with the first excited state at 27 cm⁻¹ above the ground state (Table 1).

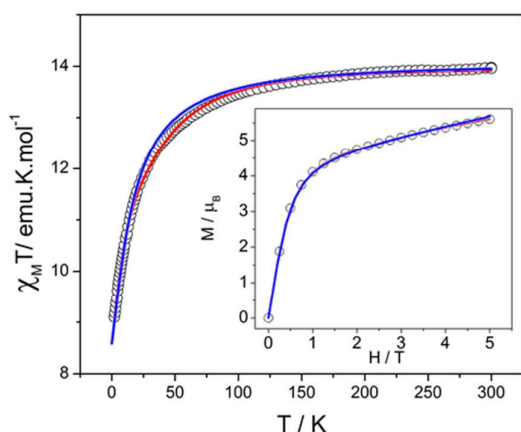


Figure 2: Temperature dependence of $\chi_M T$ and field dependence of the magnetization at 2 K (inset) with simulation based on *ab initio* calculations (blue line) and Stevens procedure considering an approximated D_{3h} symmetry (red line).

From *ab initio* calculations the calculated total splitting of the ground multiplet is 337 cm⁻¹ with the first excited state at 24 cm⁻¹ above the ground state (Tables 1 and S4-S5), in good agreement with the Stevens technique (see experimental part for computational details). However, whereas the ground state is also found to be a mixture of different M_J eigenstates, the main contributions come from the $M_J = \pm 15/2$ eigenstate. The $\chi_M T$ vs T curve is nevertheless properly reproduced (Figure 2). Such discrepancy between the two techniques is a direct consequence of considering crystallographic molecule symmetry (*ab initio*) instead of approximated first coordination sphere symmetry (Stevens).

Table 1 Energy levels extracted from Stevens procedure and *ab-initio* calculations (see SI for detailed compositions)

	Stevens procedure		Ab initio calculations	
	Energy (cm ⁻¹)	Main M_J states	Energy (cm ⁻¹)	Main M_J states
0	0	±13/2	0	±15/2
1	26.7	±11/2	24	±5/2; ±13/2
2	62.3	±1/2	52	±11/2
3	77.95	±3/2	73	±9/2
4	114.2	±5/2	99	±11/2; ±9/2
5	117.8	±9/2	165	±7/2
6	156.1	±7/2	214	±13/2; ±5/2
7	222.65	±15/2	337	±1/2

In order to investigate the magnetic relaxation of **1**, dynamic magnetic measurements (ac) were performed. Slow relaxation was observed, providing that an external dc field is applied in order to remove the zero-field fast tunnelling (Figures S5-S6).¹⁵ Field scans have been performed at 2K and the most suited dc field has been identified to be 1500 Oe. Relaxation times (τ) follows a thermally activated mechanism where $\tau = \tau_0 \exp(\Delta/k_B T)$. An energy barrier of $\Delta = 33 \pm 2$ K and a characteristic relaxation time of $\tau_0 = 5.5 \times 10^{-10}$ s are obtained¹⁶ (Figure S7 and Table S6). These results are in the range of what is commonly observed on similar compounds.¹⁴ Relaxation times distribution is quite low as observed on Cole-Cole plots^{17,18} ($\alpha = 0.21$ at 1.7 K) and almost all the molecules relax according to one mechanism (Table S7). This relaxation concerns the whole sample ($(1 - \chi_s/\chi_T) = 0.93$ at 1.7 K). It is interesting to notice that the previously reported Yb^{III} derivative shows similar energy barrier and characteristic relaxation times under comparable external dc field.¹²

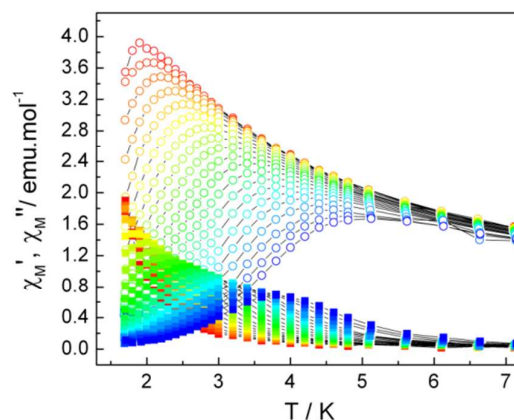


Figure 3: Temperature dependence of χ_M' (empty circles) and χ_M'' (full squares) measured with a 1500 Oe dc field and from 100 (red) to 70000 Hz (blue).

The energy barrier value is supported by *ab initio* calculations, which reveal that both the ground and first excited states have quite axial magnetic anisotropies (Table S5) but separated by an angle of 55°. This means, most likely, that the pathway for

magnetic relaxation does not reach states beyond the first excited state, which is 35 K above the ground state. This behaviour is also supported by the calculated transition moments between the different Kramer's doublets of the ground multiplet, which show efficient relaxation process already through the first excited state (Figure 4).

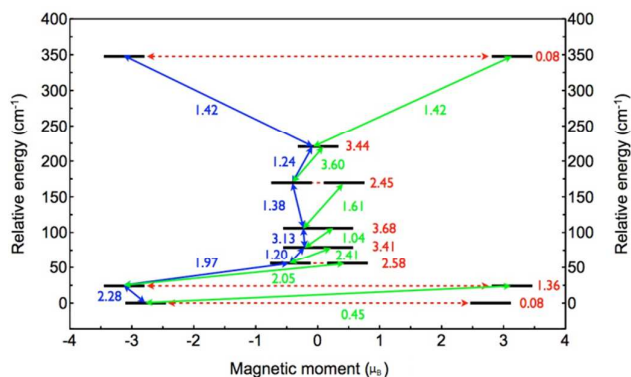


Figure 4: *Ab initio* magnetization blocking barrier, computed by mean of magnetic transition moments. The black thick lines correspond to all the spin-orbit states of **1**. The coloured arrows correspond to the different possible pathways/transitions considered in this work. The number provided at each arrow is the mean absolute value for the corresponding transition moment.

Magnetic slow relaxation on Dy^{III}-based molecules has been observed on a wide library of compounds.^{8a-c, 8f, 19} In most cases SMM behaviour is observed with a “sandwich-like” symmetry of the electrostatic surrounding of the Dy^{III}. Such geometry is the most favourable to stabilize the oblate electron density of the Dy^{III} ion and creates a sizable energy barrier for magnetic moment reversal.²⁰ *ab initio* calculations of magnetic anisotropy on **1** show that the ground state is quite axial with $g_z=16.6$ while $g_x=g_y=0.2$ (Table S5), and the associated easy-axis is oriented in the O6-O6 direction (Figures 1 and 5), *i.e.* perpendicular to the molecular C₂ axis (Dy1-N8). This evidence that local symmetry approximation based on chemical neighbouring of the metal centre (*i.e.* the three murexide ligands) is not adapted on **1** and that only crystallographic symmetries have to be considered.

Usually the easy-magnetic axis follows the «most charged» direction of the Dy^{III} surroundings.^{13a-c, 21} However in **1**, all oxygen atoms induce the same electrostatic potential on the Dy^{III} ion (Table S8) and additional contributions should be considered. This unusual case is investigated using the multipolar expansion of the electrostatic potential generated by the ligands in the close environment of the Dy^{III} ion. It is modelled using the following textbook formula:²²

$$V(M) = \sum_{i=1}^N \frac{q_i}{\|\vec{r}_i\|} + \frac{\vec{p}_i \cdot \vec{r}_i}{\|\vec{r}_i\|^3} + \frac{\vec{r}_i \cdot (\vec{Q}_i \times \vec{r}_i)}{\|\vec{r}_i\|^5} + \mathcal{O}\left(\frac{1}{\|\vec{r}_i\|^9}\right)$$

This formula defines the electrostatic potential generated by a finite distribution of charges (located at point I such as I = 1, ..., N, with N, the total number of charges in presence) in a given

point of space, here called M, located inside the latter distribution. \vec{r}_i stands for the position vector going from M to I, while q_i , \vec{p}_i and \vec{Q}_i stand for the charge, dipole moment and quadrupole moment at point I, respectively. These multipolar moments describe the spatial distribution of the charge at point I. For each considered complex, the sum over I run over all atomic positions, except the one of the lanthanide ion, and the associated multipolar moments are extracted from a LoProp calculation performed on the ground state of the system.²³ This potential is calculated in a given number of M points, equally-spaced in a sampling cube (1×1×1 Ångström³) centred on the position of the lanthanide ion. A large set of 3D data is then generated and to represent it efficiently, we use 2D maps, cut into the sampling cube along a given direction.

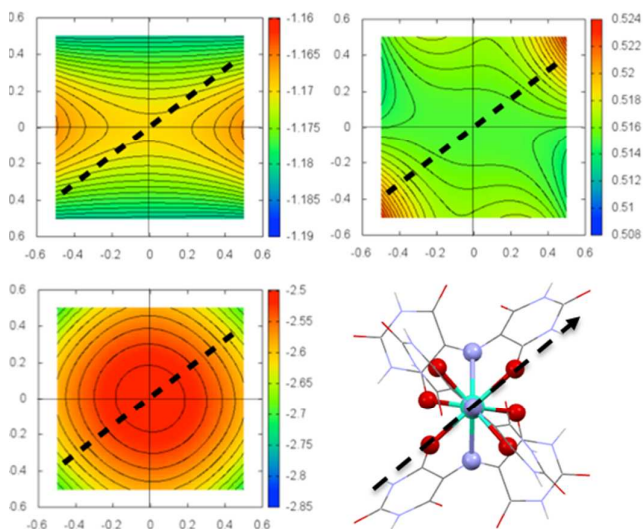


Figure 5: Mapping of the different contributions to the electrostatic potential in the plane perpendicular to the molecular C₂ axis and containing the Dy^{III} ion. Contributions are calculated in a 1 Å³ volume centred on Dy^{III} ion. The dashed black line symbolizes the orientation of the calculated ground state magnetic easy-axis. (top left) Mapping of the atomic charges, (top right) atomic dipole moments and (bottom left) atomic quadrupole moments. (bottom right) superimposition of easy magnetic axis on molecule of **1**.

Such approach permits the discrimination of the effect of atomic charges, dipole moments and quadrupole moments (Figure 5). The shape of the electrostatic potential holds a perfect C₂ axis rather than any other kind of 3-fold symmetry element. This suggests that at the lanthanide position, electrostatics are related to molecular symmetry (C₂) rather than site symmetry (D_{3h}). Going into details, the quadrupole contribution to the electrostatic potential is isotropic whereas the other two show preferential orientations. The only contribution that closely matches easy-axis direction is the dipolar one. This highlights the importance of higher order terms in the modelling of the electrostatic environment.

Conclusions

In conclusion, we have been able to synthesize the Dy^{III} adduct of the Ln(Murex)₃ family. Similarly to its Yb^{III} parent¹² it shows

a SMM behaviour. The three identical ligands generate a N_3O_6 environment around the Dy^{III} ion that in first approximation may be considered having a 3-fold symmetry. However *ab initio* calculations highlight that whereas such an approximation provide a correct splitting of energy levels and good energy barrier for spin reversal it dramatically fails in reproducing the correct wavefunction of the ground and first excited states. Similar conclusion can be made for the calculated magnetic easy-axis orientation that is not related to the 3-fold symmetry but to the crystallographic C_2 symmetry. Exploration of the various contributions to the electrostatic potential generated by the ligands around the Dy^{III} ion, shows the predominant role of the dipolar contributions. Commonly, small approximations of local symmetry around the Dy^{III} ion permit a simple and straightforward description of its magnetic properties. However this particular compound made of three equivalent ligands and very narrow bond length distribution (lower than some hundredth of Å) highlights that molecular symmetry plays a more crucial role than site symmetry in determining the shape and orientation of magnetic anisotropy.

Acknowledgements

We thank T Guizouarn for its help with magnetic measurements. XY and GH acknowledge Chinese Scholarship Council. BLG and JJ thank C. Calzado (Univ. Sevilla) for computational facilities. This work was granted access to the HPC resources of Université Aix-Marseille financed by the project Equip@Meso (ANR-10-EQPX-29-01) « Investissements d'Avenir » program supervised by the ANR.

Experimental

Materials and methods.

Synthetic Procedure: All reagents were analytical grade purchased at TCI chemicals and used as received. An aqueous solution of Murexide is reacted with $Dy(NO_3)_3 \cdot xH_2O$ salt. After some minutes a red-orange mud can be isolated by filtration. Successive washing with CH_3CN and diethyl ether provide a microcrystalline powder (85 % yield). Single crystals suitable for X-ray crystal diffraction can be isolated from the filtrate. Elemental Anal. Calcd (%) for $C_{24}H_{12}DyN_{15}O_{18}$: C 29.93, H 1.25, N 21.83; found C 27.37, H 2.10, N 19.95

Crystal Structure Determination: A Single crystal was mounted on a APEXII AXS-Bruker diffractometer equipped with a CCD camera and a graphite-monochromated $MoK\alpha$ radiation source ($\lambda=0.71073$ Å), from the Centre de Diffractométrie (CDIFX), Université de Rennes 1, France. Data were collected at 150K. Structure was solved with a direct method using the SIR-97 program²⁴ and refined with a full-matrix least-squares method on F^2 using the SHELXL-97 program²⁵ and WinGX interface.²⁶ Crystallographic data are summarized in Table S1. CCDC-1409034 contains the supplementary crystallographic data for this paper. Figure S8 gather the simulated X-ray powder diffraction pattern from this crystal structure and the experimental one obtained from the polycrystalline sample.

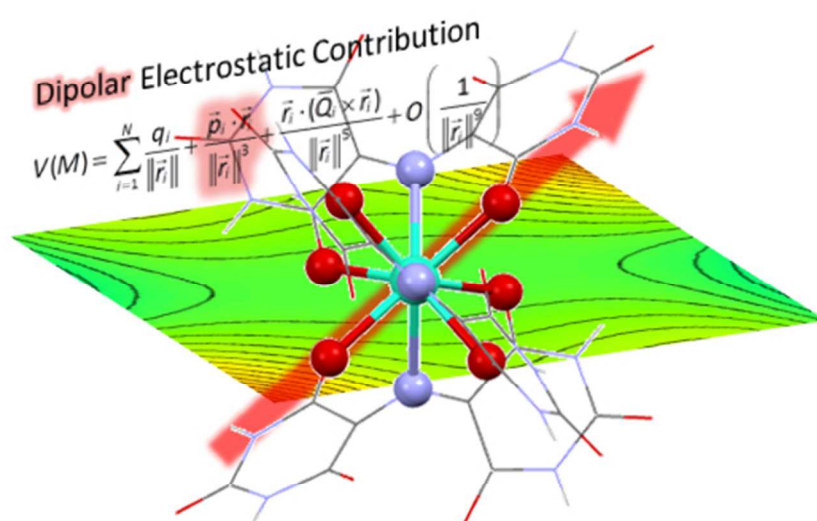
Magnetic Measurements: dc measurements were performed on a Quantum Design MPMS magnetometer. Ac measurements were measured with an homemade inductive probe; courtesy of M. Novak. All measurements were performed on polycrystalline sample embedded in grease to avoid in-field orientation of the crystallites. Measurements were corrected for the diamagnetic contribution, as calculated with Pascal's constants, and for the diamagnetism of the sample holder, as independently determined.

Computational details: To properly account for the multiconfigurational nature of the wave function of the 4f electrons of the Dy ion, the competition between the spin-orbit coupling, and the crystal-field interactions, explicitly correlated *ab initio* methods are required. Herein, the *ab initio* calculations have been carried out on the X-ray structure using MOLCAS 7.8.²⁷ In this approach the relativistic effects are treated in two steps based on the Douglas-Kroll Hamiltonian. First, the scalar terms are included in the basis set generation and are used to determine the spin-free wave functions and energies in the complete active space self-consistent field (CASSCF) method.²⁸ Next, spin-orbit coupling is added within the restricted active space state interaction (RASSI-SO) method, which uses the spin-free wave functions as basis states.²⁹ All atoms were represented by ANO-type basis sets from the ANO-RCC library. The following contractions were used: [8s7p4d3f2g1h] for the Dy ion, [4s3p2d] for the C, N and O atoms of the first and second coordination spheres, [3s2p1d] for the remaining C, N and O atoms and [2s] for the H atoms. The active space of the self-consistent field (CASSCF) method consisted of the nine 4f electrons of the central Dy ion spanning the seven 4f orbitals. For a proper description of the spin-orbit coupling on the metal site, the mixing of a large number of states is required. In the present work, state-averaged CASSCF calculations were performed for all the sextets (21 roots) of the Dy ion, all the quadruplets (224 roots) and 300 out of 490 doublets, due to hardware limitations. Since the energy spectrum of the ground multiplet (${}^6H_{15/2}$) is converged when mixing the 21 sextet roots with the 128 first quadruplet roots and the 107 first doublet roots, we make the choice not to include all possible spin-free states in the RASSI-SO calculation. The energy spectrum of the system is extracted from the RASSI-SO calculation. Using the pseudo-spin $s^{1/2}$ (« \tilde{S} » = 1/2) approximation as implemented in the SINGLE_ANISO module,³⁰ the magnetic anisotropy tensor of the 8 Kramer doublets of the ground multiplet (${}^6H_{15/2}$) are computed, as well as the temperature-dependent magnetic susceptibility, the molar magnetization at 2K and the decomposition of the wave functions of the 16 lower spin-orbit states in term of M_j eigenvectors. The atomic charges, dipolar moments and quadrupolar moments used to determine the electrostatic potential in the system are extracted from a LoProp calculation performed on the ground state of the system.²³

Notes and references

- 1 J. Ribas, *Coordination chemistry*, Wiley-vch, Weinheim, 2008.
- 2 S. Cotton, *Lanthanide and Actinide Chemistry*, 2006.
- 3 (a) L. Armelao, S. Quici, F. Barigelletti, G. Accorsi, G. Bottaro, M. Cavazzini and E. Tondello, *Coord. Chem. Rev.*, 2010, **254**, 487; (b) A. D'Aleo, F. Pointillart, L. Ouahab, C. Andraud and O. Maury, *Coord. Chem. Rev.*, 2012, **256**, 1604; (c) M. D. Ward, *Coord. Chem. Rev.*, 2007, **251**, 1663; (d) K. Binnemans,

- Chem. Rev.*, 2009, **109**, 4283; (e) Y. Cui, Y. Yue, G. Qian and B. Chen, *Chem. Rev.*, 2011, **112**, 1126; (f) A. Lan, K. Li, H. Wu, D. H. Olson, T. J. Emge, W. Ki, M. Hong and J. Li, *Angew. Chem. Int. Ed.*, 2009, **48**, 2334; (g) S. V. Eliseeva and J. C. G. Bunzli, *Chem. Soc. Rev.*, 2010, **39**, 189; (h) J.-C. G. Bunzli, *Chem. Rev.*, 2010, **110**, 2729; (i) J.-C. G. Bunzli and C. Piguet, *Chem. Soc. Rev.*, 2005, **34**, 1048; (j) A. de Bettencourt-Dias, *Luminescence of Lanthanide Ions in Coordination Compounds and Nanomaterials*, Wiley, 2014.
- 4 J. Lee, O. K. Farha, J. Roberts, K. A. Scheidt, S. T. Nguyen and J. T. Hupp, *Chem. Soc. Rev.*, 2009, **38**, 1450.
- 5 Y. Cui, H. Xu, Y. Yue, Z. Guo, J. Yu, Z. Chen, J. Gao, Y. Yang, G. Qian and B. Chen, *J. Am. Chem. Soc.*, 2012, **134**, 3979.
- 6 (a) J. Feng and H. Zhang, *Chem. Soc. Rev.*, 2013, **42**, 387; (b) A. U. Czaja, N. Trukhan and U. Muller, *Chem. Soc. Rev.*, 2009, **38**, 1284; (c) J.-C. G. Bunzli and C. Piguet, *Chem. Rev.*, 2002, **102**, 1897.
- 7 R. Sessoli, M.-E. Boulon, A. Caneschi, M. Mannini, L. Poggini, F. Wilhelm and A. Rogalev, *Nat Phys*, 2015, **11**, 69.
- 8 (a) D. N. Woodruff, R. E. P. Winpenny and R. A. Layfield, *Chem. Rev.*, 2013, **113**, 5110; (b) L. Sorace, C. Benelli and D. Gatteschi, *Chem. Soc. Rev.*, 2011, **40**, 3092; (c) R. Sessoli and A. K. Powell, *Coord. Chem. Rev.*, 2009, **253**, 2328; (d) C. Benelli and D. Gatteschi, *Chem. Rev.*, 2002, **102**, 2369; (e) P. Zhang, L. Zhang and J. Tang, *Dalton Trans.*, 2015, **44**, 3923; (f) C. Benelli and D. Gatteschi, *Introduction to Molecular Magnetism: From Transition Metals to Lanthanides*, 2015.
- 9 (a) N. Ishikawa, *Polyhedron*, 2007, **26**, 2147; (b) P. Zhang, L. Zhang, C. Wang, S. Xue, S.-Y. Lin and J. Tang, *J. Am. Chem. Soc.*, 2014; (c) Y.-N. Guo, L. Ungur, G. E. Granroth, A. K. Powell, C. Wu, S. E. Nagler, J. Tang, L. F. Chibotaru and D. Cui, *Scientific Reports*, 2014, **4**, 5471.
- 10 A. Abragam and B. Bleaney, *Electron Paramagnetic Resonance of Transition Ions*, Oxford University Press, 1970.
- 11 (a) H. E. Kaufman and E. C. Adams, *Lab. Invest.*, 1957, **6**, 275; (b) D. Davidson and E. Epstein, *J. Org. Chem.*, 1936, **1**, 305.
- 12 X. Yi, K. Bernot, V. Le Corre, G. Calvez, F. Pointillart, O. Cador, B. Le Guennic, J. Jung, O. Maury, V. Placide, Y. Guyot, T. Roisnel, C. Daiguebonne and O. Guillou, *Chem. Eur. J.*, 2014, **20**, 1569.
- 13 (a) J. Jung, F. Le Natur, O. Cador, F. Pointillart, G. Calvez, C. Daiguebonne, O. Guillou, T. Guizouarn, B. Le Guennic and K. Bernot, *Chem. Commun.*, 2014, **50**, 13346; (b) J. Jung, O. Cador, K. Bernot, F. Pointillart, J. Luzon and B. Le Guennic, *Beilstein J. Nanotechnology*, 2014, **5**, 2267; (c) T. T. da Cunha, J. Jung, M. E. Boulon, G. Campo, F. Pointillart, C. L. M. Pereira, B. Le Guennic, O. Cador, K. Bernot, F. Pineider, S. Golhen and L. Ouahab, *J. Am. Chem. Soc.*, 2013, **135**, 16332; (d) N. F. Chilton, D. Collison, E. J. L. McInnes, R. E. P. Winpenny and A. Soncini, *Nat Commun*, 2013, **4**, 2551; (e) M. E. Boulon, G. Cucinotta, J. Luzon, C. Degl'Innocenti, M. Perfetti, K. Bernot, G. Calvez, A. Caneschi and R. Sessoli, *Angew. Chem. Int. Ed.*, 2013, **52**, 350; (f) G. Cucinotta, M. Perfetti, J. Luzon, M. Etienne, P.-E. Car, A. Caneschi, G. Calvez, K. Bernot and R. Sessoli, *Angew. Chem. Int. Ed.*, 2012, **51**, 1606; (g) J. J. Baldovi, J. J. Borrás-Almenar, J. M. Clemente-Juan, E. Coronado and A. Gaita-Arino, *Dalton Trans.*, 2012, **41**, 13705.
- 14 S. T. Liddle and J. van Slageren, *Chem. Soc. Rev.*, 2015.
- 15 (a) G. Poneti, K. Bernot, L. Bogani, A. Caneschi, R. Sessoli, W. Wernsdorfer and D. Gatteschi, *Chem. Commun.*, 2007, 1807; (b) W. Wernsdorfer, N. Aliaga-Alcalde, D. N. Hendrickson and G. Christou, *Nature*, 2002, **416**, 406; (c) F. Pointillart, K. Bernot, R. Sessoli and D. Gatteschi, *Chem. Eur. J.*, 2007, **13**, 1602.
- 16 D. Gatteschi, R. Sessoli and J. Villain, *Molecular Nanomagnets*, Oxford University Press, Oxford, 2006.
- 17 H. B. G. Casimir and F. K. Du Pre, *Physica*, 1938, **5**, 507.
- 18 K. S. Cole and R. H. Cole, *J. Chem. Phys.*, 1941, **9**, 341.
- 19 F. Habib and M. Murugesu, *Chem. Soc. Rev.*, 2013, **42**, 3278.
- 20 J. D. Rinehart and J. R. Long, *Chem. Sci.*, 2011, **2**.
- 21 N. F. Chilton, S. K. Langley, B. Moubaraki, A. Soncini, S. R. Batten and K. S. Murray, *Chem. Sci.*, 2013, **4**, 1719.
- 22 D. Fleisch, *A Student's Guide to Maxwell's Equations*, Cambridge University Press, Cambridge, 2008.
- 23 L. Gagliardi, R. Lindh and G. Karlstrom, *J. Chem. Phys.*, 2004, **121**, 4494.
- 24 A. Altomare, M. C. Burla, M. Camalli, G. L. Casciarano, C. Giacovazzo, A. Guagliardi, A. G. G. Moliterni, G. Polidori and R. Spagna, *J. Appl. Crystallogr.*, 1999, **32**, 115.
- 25 G. M. Sheldrick, *Acta Crystallogr. Sect. A*, 2008, **64**, 112.
- 26 L. J. Farrugia, *J. Appl. Crystallogr.*, 2012, **45**, 849.
- 27 F. Aquilante, L. De Vico, N. Ferre, G. Ghigo, P. Å. Malmqvist, P. Neogrady, T. B. Pedersen, M. Pitonak, M. Reiher, B. O. Roos, L. Serrano-Andres, M. Urban, V. Veryazov and R. Lindh, *J. Comput. Chem.*, 2010, **31**, 224.
- 28 B. O. Roos, P. R. Taylor and P. E. M. Siegbahn, *Chem. Phys.*, 1980, **48**, 157.
- 29 (a) P.-Å. Malmqvist and B. O. Roos, *Chem. Phys. Lett.*, 1989, **155**, 189; (b) P. Å. Malmqvist, B. O. Roos and B. Schimmelpfennig, *Chem. Phys. Lett.*, 2002, **357**, 230.
- 30 L. F. Chibotaru and L. Ungur, *J. Chem. Phys.*, 2012, **137**.



A DyIII-based single-molecule magnet is reported. *ab initio* calculations highlight that molecular symmetry plays a predominant role over site symmetry in determining the shape and orientation of DyIII magnetic anisotropy. Moreover the dipolar component of the electrostatic potential created by the surrounding ligands is shown to be the driving force of its magnetic behaviour.